JACS Au
AN OPEN ACCESS JOURNAL OF THE AMERICAN CHEMICAL SOCIETY

pubs.acs.org/jacsau
Article

Dicationic 1-Germa and 1-Stannavinylidenes: Synthesis, Structure, and Reactivity

Yuankai Li,[†] Huan Mu,[†] Zhuchunguang Liu,[†] Zexin Qi, Jiliang Zhou, and Zhaowen Dong*

Cite This: *JACS Au* 2025, 5, 1289−1298
Read Online

ACCESS | Metrics & More | Article Recommendations | Supporting Information

ABSTRACT: The synthesis of heteronuclear vinylidene analogues containing heavier group 14 elements ($R_2C{=}E{:}$, E = Si, Ge, Sn) has been a challenging task due to their inherent instability. In this study, we report the synthesis of dicationic 1-germavinylidene (**3Ge**) and 1-stannavinylidene (**3Sn**) by using sym-bis(2-pyridyl)-tetraphenylcarbodiphosphorane ($CDPPy_2$) as a donor ligand. Both **3Ge** and **3Sn** have been characterized by single-crystal X-ray diffraction analysis, NMR spectroscopy, and high-resolution mass spectrometry. The structural analysis, supported by the results of theoretical calculations, confirms that **3Ge** and **3Sn** feature a polarized C═E double bond and a lone pair of electrons located at the E atom (E = Ge and Sn). The reactions of **3Ge** with IDippMCl (M = Cu, Ag, Au) give the M−Cl bond addition products. Mechanistic studies on the activation of the Au−Cl bond by **3Ge** demonstrate its ambiphilicity. This work represents an example of the utilization of a carbone ligand as both an σ and π donor for the synthesis of heavier heteronuclear vinylidene analogues.

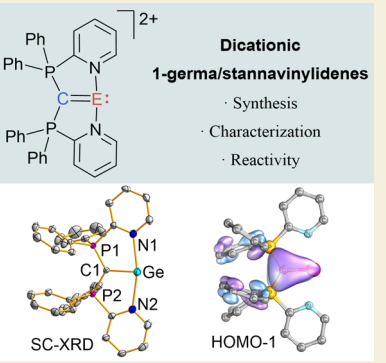

KEYWORDS: *germanium, tin, main group compound, multiple bonds, single-crystal X-ray diffraction*

INTRODUCTION

Vinylidenes with the general formula of $R^1R^2C{=}C{:}$ (**A**), which contain a carbon−carbon double bond, are isomers of alkynes (Figure 1a).[1,2] They represent an important class of unsaturated carbenes and are recognized as crucial reactive intermediates in organic reactions, thereby becoming an integral part of the field of organic chemistry.[2] Replacing the carbon atoms of the double bond of vinylidenes with heavier group 14 elements such as silicon, germanium, and tin leads to heavier vinylidene analogues **B** ($R^1R^2E{=}E'{:}$, E and E′ = Si, Ge, Sn, Figure 1a).[3] These heavier vinylidene analogues exhibit unique reactivity, which is attributed to their distinctive electron configuration featuring a lone pair of electrons, an empty p-orbital, and an unsaturated E═E′ double bond. In 2013, the Scheschkewitz group reported the isolation of the first Lewis base-stabilized silagermenylidene, using N-heterocyclic carbene (NHC) as a donor ligand.[4] This breakthrough opens the door to the exploration of Lewis base-stabilized heavier vinylidene analogues.[5] Subsequent work by the Filippou, Iwamoto, Mo, and Wesemann groups resulted in the synthesis and isolation of NHC, N-heterocyclic silylene (NHSi), and phosphine-stabilized heavier vinylidene analogues.[6] Notably, Aldridge et al. isolated and characterized a base-free digermavinylidene with a σ-electron donating boryl group ($[(HCDippN)_2B]_2Ge{=}Ge{:}$).[7]

By substituting one carbon atom in vinylidene with a heavier group 14 element, their heteronuclear analogues, namely, 2-sila, 2-germa, and 2-stannavinylidenes **C** ($R^1R^2E{=}C{:}$, E = Si, Ge, Sn) and 1-sila, 1-germa, and 1-stannavinylidenes **D** ($R^1R^2C{=}E'{:}$, E = Si, Ge, Sn) are acquired (Figure 1a).[3a,8] For the Lewis base-stabilized heteronuclear analogues **C** and **D**, only few examples have been reported to date.[9−11] Two decades ago, Leung et al. reported the base-stabilized oligomeric heterovinylidenes.[9] So and Sindlinger groups reported the NHC-stabilized 1-silavinylidene **I** and **II**, respectively (Figure 1b).[10,11] Very recently, Das and Filippou et al. prepared the NHC-stabilized 2-sila and 2-germavinylidenes **III** (Figure 1b).[12] However, monomeric 1-germa and 1-stannavinylidenes have not been synthesized and isolated due to their inherent instability.

Carbodiphosphoranes (CDPs), also known as carbones, possess two orthogonal σ and π lone pairs at the center carbon (C^0).[13] Latest studies show that CDPs can serve as double-dative ligands, with the two lone pairs on the central carbon atom being capable of simultaneously coordinating to the same metal or main group center, thus forming double-bonded compounds.[14,15] Inspired by this finding, we propose that the heteronuclear vinylidene analogues can be readily obtained by combining the CDP ligands with E^{2+} dications (E = Si, Ge, or Sn). To further improve the stability of the target compounds, we selected the tridentate sym-bis(2-pyridyl)-tetraphenylcar-

Received: November 25, 2024
Revised: February 13, 2025
Accepted: February 13, 2025
Published: February 19, 2025

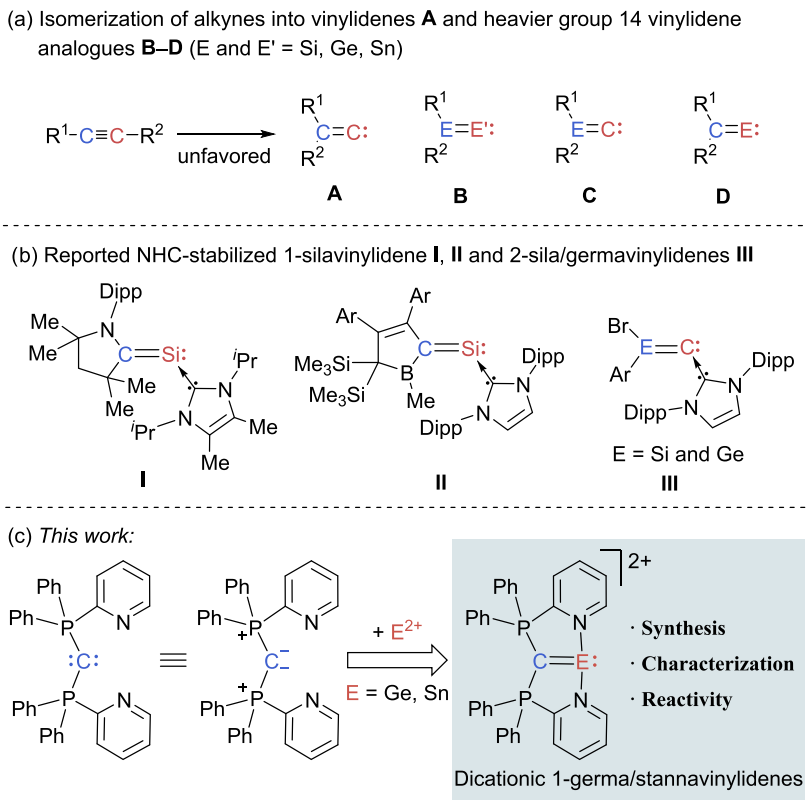

Figure 1. (a) Isomerization of alkynes and their heavy group 14 analogues into vinylidenes and heavier group 14 vinylidene analogues (**A**–**D**); (b) selected examples of reported NHC-stabilized heteronuclear vinylidene analogues containing heavier group 14 elements (**I**–**III**); (c) dicationic 1-germanvinylidene and 1-stannavinylidene reported in this work.

bodiphosphorane ($CDPPy_2$) ligand, which features pyridine groups that can coordinate to the central heavier group 14 elements (Figure 1c).[16] Utilizing this approach, we are able to synthesize and isolate a new class of stable dicationic 1-germavinylidene and 1-stannavinylidene in a single step (Figure 1c).

RESULTS AND DISCUSSION

The synthesis of $CDPPy_2$ supported chlorogermyliumylidene **2Ge** was accomplished through a direct reaction between equivalent amounts of $CDPPy_2$ and $GeCl_2$·dioxane in Et_2O (Scheme 1a).[14b] **2Ge** was isolated as a yellow solid in 73% yield on a gram scale. Addition of trimethylsilyl trifluoromethanesulfonate (Me_3SiOTf) to Et_2O solution of **2Ge** resulted in the formation of dication **3Ge** as a pale yellow solid in a yield of 85% (Scheme 1b). A one-pot approach involving the in situ addition of TMSOTf to a mixture of $GeCl_2$·dioxane and $CDPPy_2$ could also be used to prepare **3Ge**, achieving a yield of 82% (Scheme 1c). The tin analogue **3Sn** could be synthesized by a similar method. The two-step synthesis of **3Sn** resulted in a combined yield of 65% (Scheme 1a,b). The one-pot synthesis of **3Sn**, however, yielded an NMR yield of only 33%, with the byproduct being challenging to separate (Scheme 1c). Compounds **2E** and **3E** (E = Ge, Sn) were characterized by NMR spectroscopy and high-resolution mass spectrometry (HRMS) analysis. **2Ge**, **3Ge**, and **3Sn** in the solid state were further determined by single-crystal X-ray diffraction (sc-XRD) analysis (Figure 2; for details, see the Supporting Information).

The ^{13}C NMR chemical shifts of the central C1 atoms of the $CDPPy_2$ ligand in **2Ge** (16.5 ppm) and **2Sn** (20.3 ppm) are shifted downfield compared to that of the $CDPPy_2$ ligand ($\delta^{13}C$ = 12.1 ppm) (Table S4). This is quite common when

Scheme 1. Synthesis of Compounds 3Ge and 3Sn[a]

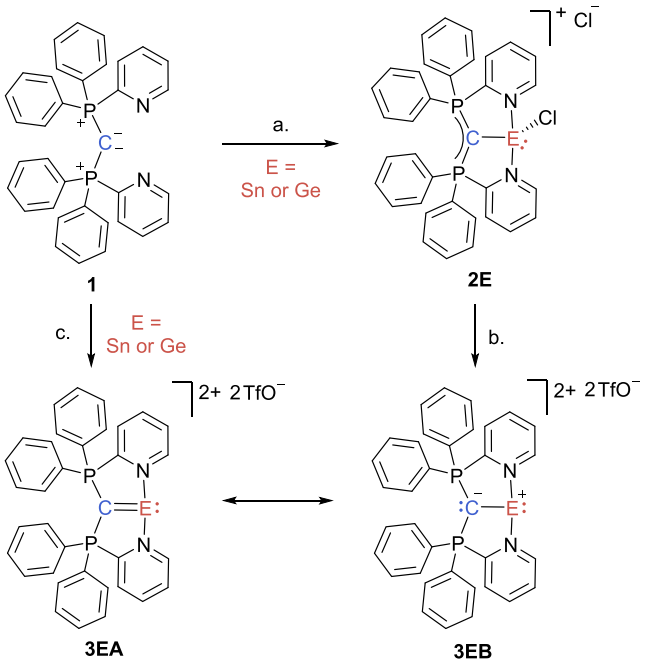

[a]Reagents and conditions: (a) $GeCl_2$·dioxane or $SnCl_2$ (1 equiv), Et_2O, 12 h, room temperature (rt); (b) Me_3SiOTf (2.5 equiv), Et_2O, 12 h, −30 °C to rt; (c) $GeCl_2$·dioxane or $SnCl_2$ (1 equiv), then Me_3SiOTf (2.5 equiv), Et_2O, 12 h, −30 °C to rt.

https://doi.org/10.1021/jacsau.4c01139
JACS Au 2025, 5, 1289−1298

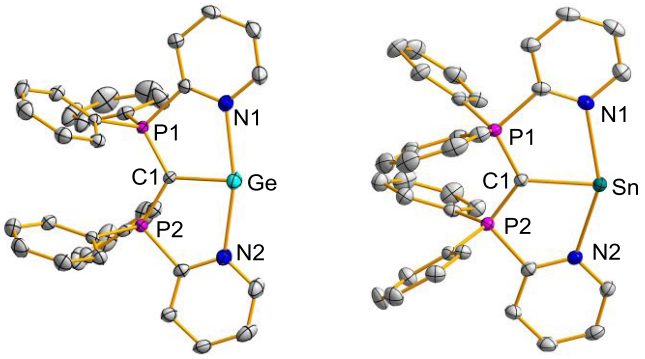

Figure 2. Molecular structures of **3Ge** and **3Sn**. Left: Structure of **3Ge** in the crystal. Selected bond length (Å) and angle (deg) for **3Ge**: C1−P1: 1.716(4), C1−P2: 1.712(4), C1−Ge: 1.977(5), Ge−N1: 2.341(4), Ge−N2: 2.247(3); P1−C1−P2: 119.4. Right: Structure of **3Sn** in the crystal. Selected bond length (Å) and angle (deg) for **3Sn**: C1−P1: 1.697(3), C1−P2: 1.699(2), C1−Sn: 2.208(2), Sn−N1: 2.493(2), Sn−N2: 2.470(2); P1−C1−P2: 119.8. Hydrogen atoms, solvents, and OTf^- anions were omitted for clarity. Thermal ellipsoids are set at the 50% probability level.

$CDPPy_2$ acts as a σ-donor ligand, as exemplified by the ^{13}C NMR signal at 11.3 ppm for the identical carbon atom in the palladium complex $[(CDPPy_2)PdCl]Cl$.[16] The ^{13}C NMR spectra of dications **3Ge** and **3Sn** exhibit resonances at 121.7 and 125.6 ppm for the central C1 atoms of the $CDPPy_2$ ligand, which are significantly shifted downfield compared to the corresponding starting materials **2Ge** and **2Sn** ($\delta^{13}C$ = 16.5 and 20.3 ppm). However, these values are very close to the range of the ^{13}C NMR resonances reported for germenes and stannenes with Ge=C and Sn=C double bonds ($\delta^{13}C$ = 130−160 ppm).[17] Furthermore, the ^{119}Sn NMR spectrum of **3Sn** presents one singlet at −87.9 ppm, which is shifted upfield by comparison with that observed for **2Sn** (−34.2 ppm). The results of NMR analyses of the dications **3Ge** and **3Sn** provide the first evidence for the presence of double-bond character between the C atom and the E (E = Ge, Sn) atom.

Graphic representations of the structures of **3Ge**, **3Sn**, and **2Ge** in the crystal are shown in Figures 2 and S8−S10. As expected, the two N and C1 donor sites of the rigid tridentate $CDPPy_2$ ligand coordinate to the Ge center in **3Ge**, resulting in a T-shaped $CDPPy_2$-Ge complex. The Ge···O distances (2.247(3) and 2.923(4) Å) between Ge atom and the O atom of the counteranion OTf^- in **3Ge** are significantly longer than the typical length of the Ge−O covalent bond (1.75−1.85 Å)[18] and the weak Ge−O bond (2.03 Å) in NHC → [GeClOTf] (Figure S9).[19] This indicates that the interaction between the Ge atom and the O atom in **3Ge** is very weak or even nonexistent.[20] The N−Ge bond distances (2.341(4) and 2.350(4) Å) fall within the range observed for the multidentate N-ligand stabilized Ge(II) cations (varying from 2.05 to 2.32 Å), suggesting the N → Ge donor−acceptor interaction.[21] The GeCP1N1 and GeCP2N2 five-membered rings in **3Ge** are nearly coplanar. This conformation favors σ and π donation between the C1 and Ge atoms. The Ge−C1 bond length (1.977(5) Å) in **3Ge** is shortened relative to what were found for **2Ge** (2.018(5) Å) and CDP → $GeCl_2$ (2.063 Å) reported by the group of Alcarazo[14b] but is slightly longer than typical Ge=C double bond (1.78 Å)[22] and the reported C=Ge double bonds (varying from 1.81 to 1.93 Å).[17] We noted that this value is very close to the reported C=Ge double bond in CDP−$[GeCl]^+$ cation (1.954 Å).[14b] These data indicate the presence of multiple bonds between the C1 and Ge atoms in **3Ge**. Similar bonding situations were also observed in the tin analogue **3Sn** (Figure 2 and Table 1). The Sn−C1 bond length

Table 1. Selected Bond Lengths (Å) and Angles (Deg) and Experimental ^{13}C NMR Chemical Shifts (ppm) of Compounds 2Ge, 3Ge, 3Sn, and 4

	2Ge	3Ge	3Sn	4
C1−E[a]	2.018(3)	1.977(5)	2.208(2)	1.933(7)
C1−P1	1.696(3)	1.716(4)	1.699(2)	1.721(11)
C1−P2	1.694(2)	1.712(4)	1.697(3)	1.712(9)
E−O1[a]		2.247(3)	2.413(2)	
E−O2[a]		2.923(4)	2.828(2)	
E−N1	2.497(3)	2.350(4)	2.493(2)	2.216(9)
P1−C1−P2	123.7(2)	119.4(2)	119.8(3)	125.4(6)
N1−E−N2	157.1(8)	163.1(1)	152.3(7)	166.1(3)
$\delta^{13}C$ (C1)[b]	16.2	121.7	125.6	122.2

[a]E = Ge or Sn. [b]Data were recorded in dichloromethane-d_2 (DCM-d_2).

in **3Sn** is 2.208 Å, which is similar to that found for the dimer of CDP−$[SnCl]^+$ (2.201 Å), but shorter than the Sn−C bond observed for the 4-dimethylaminopyridine stabilized CDP−$[SnCl]^+$ (2.272 Å).[14b]

To elucidate the electronic structures of **3Ge** and **3Sn**, density functional theory (DFT) calculations were performed at the BP86-D3(BJ)/def2-TZVP level.[23] The calculated structures for **3Ge** and **3Sn** are very close to the molecular structures determined by sc-XRD analysis (Table S6). The highest occupied molecular orbital (HOMO) is a predominantly in-plane σ lone pair orbital located on the Ge atom (Figure 3). The HOMO−1 consists of an out-of-plane π-orbital of the C1=Ge bond strongly polarized toward the carbon atom, while the lowest unoccupied molecular orbital (LUMO) is a π^*-orbital. The HOMO−12 features substantial contributions from the σ-bonding orbital for the C1−Ge bond. This unambiguously demonstrates the double-bond character of the C1=Ge bond in **3Ge**, which is consistent with the discussion of the structural parameters. Additionally, the HOMO−15 indicates the N → Ge donor−acceptor interaction. Similar molecular orbitals were also observed in **3Sn** (Figure S18). Overall, frontier molecular orbital (FMO) analysis reveals the double-bond character of the C=E bond in **3E** (E = Ge and Sn) and the presence of ambiphilic E centers.

The natural bond orbital (NBO) calculations for **3Ge** and **3Sn** were conducted to further illustrate the bonding situation.[24] According to the NBO analysis, the amount of C1 → E (E = Ge, Sn) σ-donation is evaluated to be 0.40 *e* for **3Ge** and 0.36 *e* for **3Sn** (for details, see Figures S19 and S21). Remarkably, the C1=Ge π-bonding orbital in **3Ge** is significantly polarized toward the C1 atom (orbital contributions: C1: 87%; Ge: 13%) (Figure S19). The amount of the C1 → Sn π interaction for **3Sn** is estimated to be 0.21 *e* (Figure S21). The NBO analysis of **3Ge** and **3Sn** undoubtedly demonstrates the double-bond character between the C1 atom and the E (E = Ge and Sn) atom, and the π−electron negative hyperconjugation analyses are shown in Figures S20 and S22.[25] The Ge and Sn atoms in **3Ge** and **3Sn** contain a nonbonding in-plane lone pair orbital with mainly s character (s: 89.1%, p: 10.9% (**3Ge**) and s: 90.9%, p: 9.1% (**3Sn**)). Furthermore, the calculated Wiberg bond index (WBI) for the C1−Ge bond in

https://doi.org/10.1021/jacsau.4c01139
JACS Au 2025, 5, 1289−1298

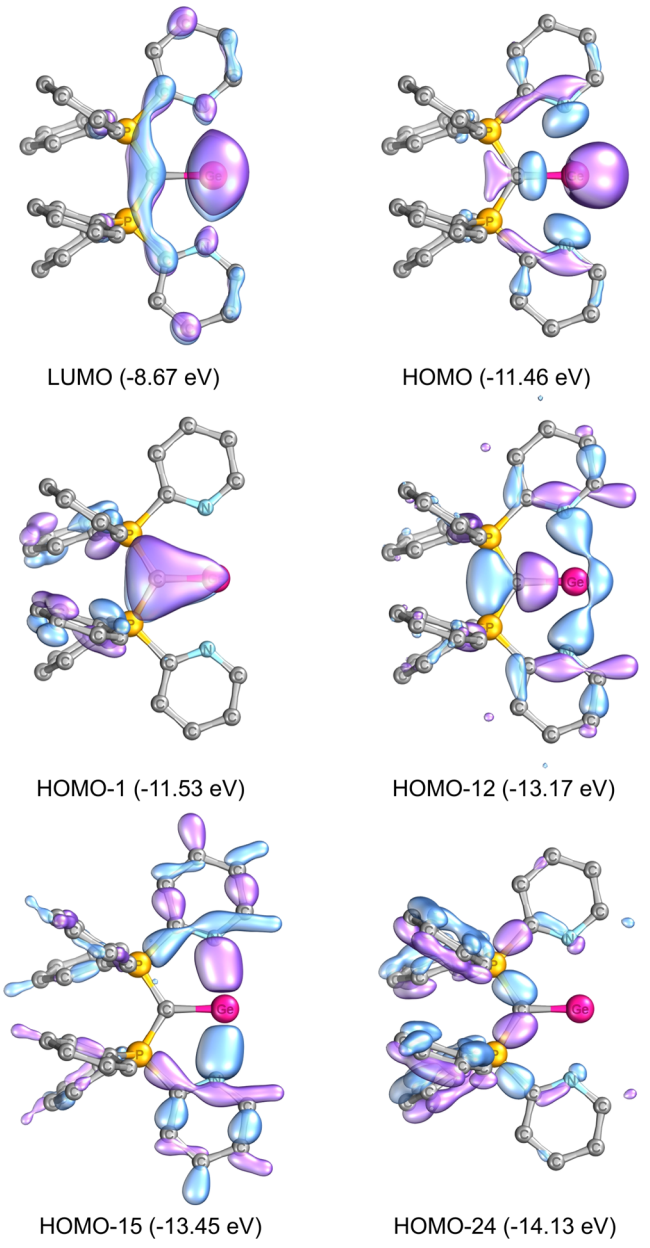

Figure 3. Selected frontier molecular orbital of **3Ge** (calculated at the BP86-D3(BJ)/def2-TZVP level and isodensity value of 0.04).

3Ge is 0.93, and the corresponding value for the C1−Sn bond in **3Sn** is 0.79.[26] The calculated WBI values for C1−E (E = Ge and Sn) in **3Ge** and **3Sn** are higher than what were reported for the previously reported CDP−$[ECl]^+$ cation (E = Ge and Sn) (WBI = 0.84 (Ge) and 0.49 (Sn)).[14b] This suggests that the σ- and π-donation in **3Ge** and **3Sn** is relatively stronger compared to the CDP−$[ECl]^+$ species. The NPA charges of the Ge and Sn atoms for **3Ge** and **3Sn** are +1.10 and +1.22 au individually, while those of C1 are −1.56 and −1.57 au (Figure S15). This implies a higher degree of polarization of the C1−E bonds, which is in agreement with the results of the MO and NBO analysis.

The extended transition state-natural orbitals for chemical valence (EST-NOCV) analysis reveals that the dominant orbital interactions in **3Ge** correspond to the C1 → Ge σ/π-donation (NOCV pairs 1 and 2) and N → Ge σ-donation (NOCV pair 3) with stabilization energies of −97.14/−29.07 and −32.71 kcal/mol, respectively (Figures 4 and S30).[27] Notably, the C1 → Ge σ-donation in **3Ge** is substantially

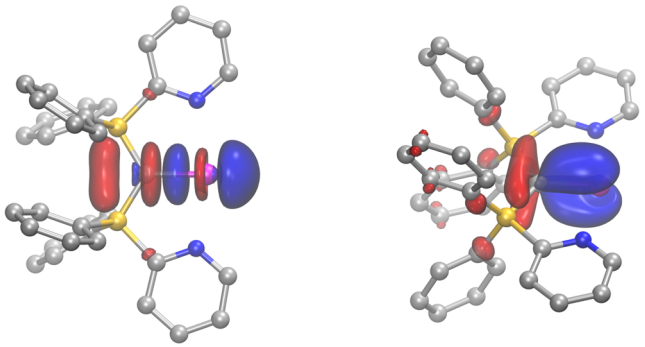

Figure 4. ETS-NOCV analysis of **3Ge** (calculated at the BP86-D3(BJ)/def2-TZVP//BP86-D3(BJ)/def2-TZVP level; charge flows from red to blue).

stronger than the corresponding π-donation, which is in line with the NBO analysis. Similar results were obtained for **3Sn** (Figure S31).

Thereafter, the electron density for **3Ge** and **3Sn** was analyzed using the quantum theory of atom in molecules (QTAIM) method (Figures 5 and S26−S29).[28] The results of QTAIM analysis reveal that the P−C1 bond in **3Ge** and **3Sn** is an electron-sharing covalent bond as the bond critical point (BCP) with a negative $\nabla^2\rho(r_c)$ and negative total energy density ($H(r_c)$). The C1−E (Ge and Sn) can be regarded as a polar covalent bond, given that their BCPs are situated in close proximity to a nodal surface of the Laplacian $\nabla^2\rho(r_c)$ and exhibit positive $\nabla^2\rho(r_c)$ and negative $H(r_c)$ values. The ellipticity values ($\varepsilon(r_c)$) at the BCP of C1−E bonds are 0.20 (E = Ge) and 0.17 (E = Sn), respectively, which are substantially larger than zero, thereby further supporting the presence of the double-bond character of C1−E bonds (E = Ge or Sn). The electron localization function (ELF) analysis again verifies the presence of a lone pair at Ge and Sn atoms and covalent bonding between E and C1 atoms in **3Ge** and **3Sn** (Figure S16).[29]

We conducted the energy decomposition analysis (sobEDA) to investigate in depth the bonding nature of the E−C bonds (E = Ge or Sn) in **3Ge** and **3Sn**, aiming to determine whether the double bonds are better described as electron-sharing double bonds or as σ and π dative bonds.[30] The magnitude of the absolute value of the orbital term $|\Delta E_{orb}|$ serves as a valuable metric for classifying bond types (Tables 2 and S9). The sobEDA results of **3Ge** show that the value of $|\Delta E_{orb}|$ between the triplet fragments (317.80 kcal/mol) is lower than that between the singlet fragments (370.05 kcal/mol) and between the doublet fragments (330.22 kcal/mol). Consequently, **3Ge** should be described as electron-sharing σ and π bonds (as depicted in Scheme 1, **3GeA**). Conversely, the calculated $|\Delta E_{orb}|$ value for the doublet−doublet combination for **3Sn** (270.95 kcal/mol) is significantly smaller than that of the singlet−singlet combination (300.93 kcal/mol) and triplet−triplet combination (327.81 kcal/mol), indicating the presence of an electron-sharing σ bond and a dative π bond between the Sn and C atoms in **3Sn** (as depicted in Scheme 1, **3SnB**).

https://doi.org/10.1021/jacsau.4c01139
JACS Au 2025, 5, 1289−1298

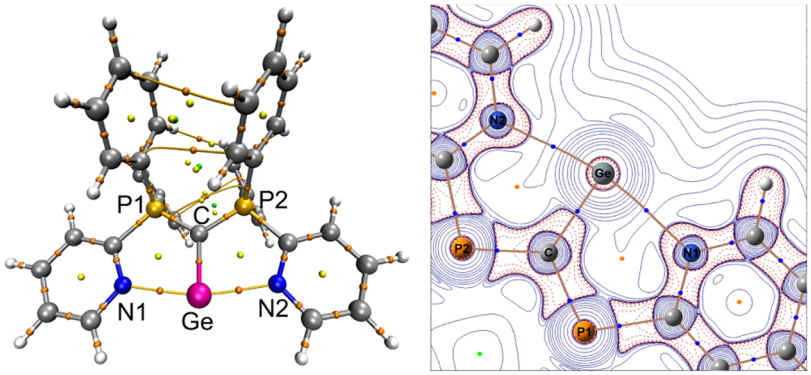

Figure 5. Left: molecular graph of **3Ge** based on QTAIM analysis. Gray lines indicate bond paths, orange circles represent bond critical points, and yellow circles represent ring critical points. Right: part of the molecular graph of **3Ge** was projected on a contour plot of the Laplacian of the electron density ($\nabla^2\rho(r_c)$) in the GeCP2 plane (calculated at the BP86-D3(BJ)/def2-TZVP level).

Table 2. sobEDA Analysis Results for 3Ge and 3Sn, Calculated at the B3LYP-D3(BJ)/def2-TZVP Level[a]

	3Ge		3Sn	
	$CDPPy_2$ (S) + Ge^{2+} (S)	$CDPPy_2^{2+}$ (T) + Ge (T)	$CDPPy_2^{+}$ (D) + Sn^{+} (D)	$CDPPy_2^{2+}$ (T) + Sn (T)
ΔE_{int}[b]	−391.68	−178.47	−116.76	−172.17
ΔE_{xrep}[c]	250.77	389.35	297.36	340.10
ΔE_{els}[d]	−246.33 (40.0%)	−209.91 (39.8%)	−109.12 (28.7%)	−145.06 (30.7%)
ΔE_{orb}[d]	−370.05 (60.0%)	−317.80 (60.2%)	−270.95 (71.3%)	−327.81 (69.3%)
ΔE_c[e]	−26.06	−40.12	−34.05	−39.41

[a]Energy values are given in kcal/mol. S = singlet, D = doublet, and *T* = triplet. [b]Total interaction energy. [c]Exchange energy and Pauli repulsion energy. [d]Percentage contribution to the total attractive interactions ΔE_{els} + ΔE_{orb}. [e]DFT correlation energy and dispersion correction energy.

The reactivity of **3Ge** was further investigated as an illustrative example, given its parallel electronic configuration to that of **3Sn**. The potential of **3Ge** as an ambiphilic species for bond activation has been studied. We examined the reactions of **3Ge** toward the coinage metal complexes, IDippMCl (M = Cu, Ag, and Au; IDipp = 1,3-bis(2,6-diisopropylphenyl)imidazol-2-ylidene). The reaction of **3Ge** with IDippAuCl in *o*-dichlorobenzene (*o*-DCB) at room temperature gave the Au−Cl addition product **4** in a yield of 80% (Scheme 2). However, for the reactions of **1-Ge** with IDippAgCl and IDippCuCl, the novel di- and tricoordinated silver and copper complexes **5** and **6** were synthesized in good yields. Complexes **4**−**6** are characterized by NMR spectroscopy and sc-XRD analysis. The DFT calculations show that the reaction of **3Ge** with IDippAuCl proceeds via a concerted pathway rather than an electrophilic pathway (for details, see Figure S32). This indicates the ambiphilic character of **3Ge**, which is in agreement with the FMO analysis.

The solid-state structures of **4**−**6** are depicted in Figure 5. The pentacoordinate germanium in **4**−**6** adopts a trigonal bipyramidal coordination environment. The Ge−Au−C^{NHC} bond angle in **4** is 175.80(2)°, indicating a linear arrangement of the three atoms (Figure 6a). The silver ion in **5** is coordinated with two $CDPPy_2Ge^{II}Cl$ ligands with a Ge−Ag−Ge bond angle of 146.7(2)° (Figure 6b). In addition, the two $[TfO]^-$ anions are close to the silver atom (the distance between the two O atoms and the Ag atom is 2.537(9) Å). This close proximity causes the Ge−Ag−Ge angle to deviate from linearity by 33.3°, thus reducing the steric hindrance between the $[TfO]^-$ anion and $CDPPy_2Ge^{II}Cl$ ligands. Whereas the Cu ion in **6** is bound by three $CDPPy_2Ge^{II}Cl$ ligands, and the three Ge atoms and the Cu atom are nearly coplanar (Figure 6c). It is worth pointing out that compound **6** is the first structurally characterized copper complex exclusively coordinated by three Ge^{II} ligands.[31] The disparity in the coordination environment of coinage metals (Au, Ag, and Cu) may arise from differences in their atomic radius and electronegativity. The Ge−Au (2.338(1) Å), Ge−Ag (2.476(1) Å), and Ge−Cu (2.370(1) Å) bonds in **4**−**5** fall into the range of what were reported for Ge^{II} ligated Au, Ag, and Cu complexes.[31]

CONCLUSIONS

To conclude, we have reported the synthesis and isolation of novel dicationic 1-germavinylidene (**3Ge**) and 1-stannavinylidene (**3Sn**) by using the $CDPPy_2$ ligand as both *σ*- and *π*-donors. Structural and theoretical analyses have shown that these compounds feature a polarized double C═E bond with a lone pair on the E atom (E = Ge or Sn). The analysis also highlighted the presence of a robust *σ* bond and a relatively weaker *π* component in the C═E bond, which is attributable to the polarization of the C═E double bond. The reactivity of **3Ge** was examined with coinage metal complexes IDippMCl (M = Cu, Ag, Au), leading to the formation of M−Cl addition products **4**−**6**. The DFT calculations for the reaction mechanism indicate the ambiphilic character of **3Ge**. Further studies are underway in our laboratory to explore the reactivity and catalytic potential of these complexes.

MATERIALS AND METHODS

Materials

All reactions were performed under a controlled dry argon or nitrogen atmosphere using a high-vacuum line, standard Schlenk techniques, and a Vigor glovebox. The glassware was dried in an oven at 120 °C and evacuated prior to use. The solvents tetrahydrofuran (THF), diethyl ether (Et_2O), benzene, and *n*-hexane were dried over sodium/potassium alloy and distilled under argon prior to use. Toluene was

https://doi.org/10.1021/jacsau.4c01139
JACS Au 2025, 5, 1289−1298

Scheme 2. Synthesis of Compounds 4–6[a]

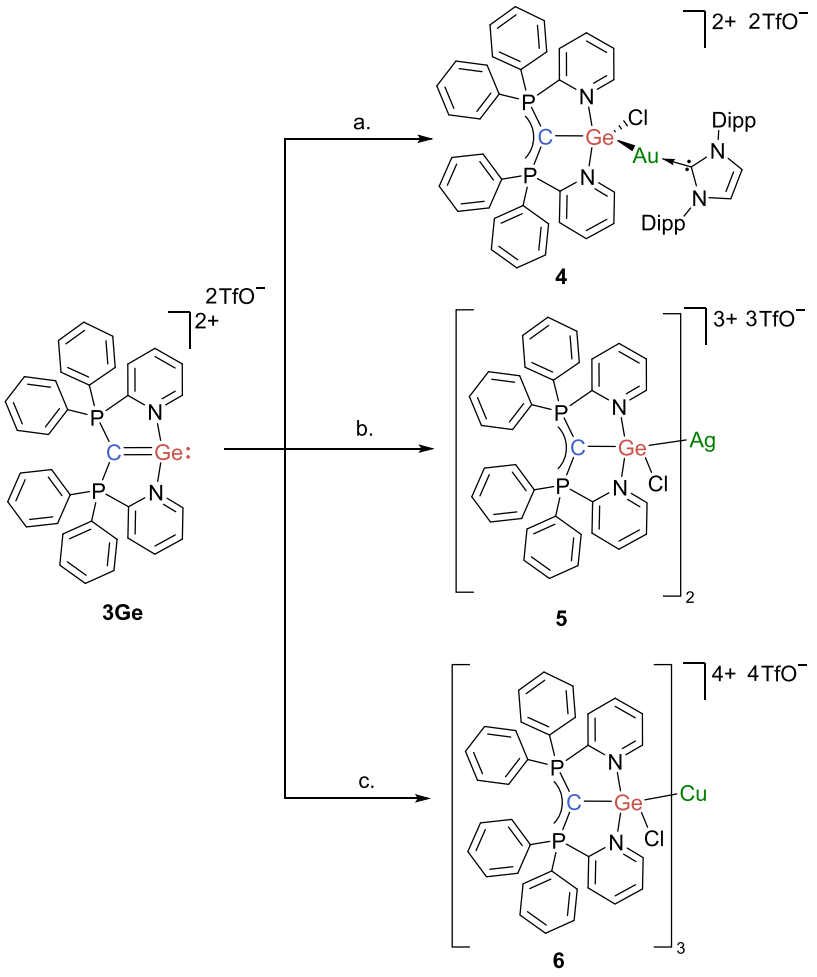

[a]Reagents and conditions: (a) DippNHC-AuCl (1 equiv), *o*-DCB, 12 h, rt; (b) DippNHC-AgCl (1 equiv), *o*-DCB, 12 h, rt; (c) DippNHC-CuCl (1 equiv), *o*-DCB, 12 h, rt.

dried over sodium and distilled under argon prior to use. *ortho*-Dichlorobenzene was dried over a 4 Å molecular sieve. Dichloromethane (DCM) was dried over calcium hydride and distilled under argon prior to use. Deuterated benzene (C_6D_6) was dried over sodium/potassium alloy, distilled, and stored over a molecular sieve (4 Å). Dichloromethane-d_2 was dried over CaH_2, distilled, and stored over a molecular sieve (4 Å). All used standard chemicals were purchased from Energy Chemical, Bidepharm, Keshi, Damas-β, J&K, TCL, or Sigma-Aldrich and used as delivered if not mentioned otherwise. Sym-bis(2-pyridyl)-tetraphenylcarbodiphosphorane ($CDPPy_2$)[16] was prepared according to the procedure described in the literature.

Analytical Methods

NMR spectra were recorded on Bruker AVANCE III HD 400 NMR spectrometers. All NMR spectra were acquired at 298 K unless otherwise specified. Multiplets were assigned as s (singlet), d (doublet), t (triplet), dd (doublet of doublet), and m (multiplet). ^{1}H NMR spectra were calibrated against the residual proton signal of the solvent as an internal reference (benzene-d_6: δ^1H = 7.16; dichloromethane-d_2: δ^1H = 5.32) and ^{13}C{^{1}H} NMR spectra by using the central line of the solvent signal (benzene-d_6: δ^{13}C = 128.0; dichloromethane-d_2: δ^{13}C = 53.8). The ^{31}P NMR spectra were calibrated using an external standard (δ^{31}P (H_3PO_4) = 0.0) and ^{19}F NMR spectra against external $CFCl_3$ (δ^{19}F ($CFCl_3$) = 0.0). The ^{119}Sn{^{1}H} NMR spectra were a reference to an external standard Me4Sn (δ^{119}Sn (Me_4Sn) = 0.0).

High-resolution mass spectra (HRMS) analyses were recorded on the exactive mass spectrometer (Thermo Scientific, USA) equipped with an electrospray ionization (ESI) ionization source.

X-ray Crystallography

A suitable crystal was detected on a Bruker D8 Venture diffractometer. The crystal was kept at 150.0 K during data collection. The solutions and refinements of the structures were performed by the latest available versions of ShelXT[32] and ShelXL.[33] Crystallographic data have been deposited with the Cambridge Crystallographic Data Centre and correspond to the following codes: CCDC—2375524 (**3Ge**), CCDC—2375526 (**3Ge**), CCDC—2375525 (**3Sn**), CCDC—2375527 (**4**), CCDC—2375529 (**5**), and CCDC—2375528 (**6**).

Computational Methods

All calculations were carried out by using the Gaussian16[23] suite of computational programs. Geometry optimizations of all structures were achieved using BP86-D3(BJ) functional.[34,35] The standard def2-TZVP and def2-SVP basis sets were applied for all atoms.[36] Frequency calculations were also conducted at the same level of theory to obtain vibrational frequencies to determine the identity of stationary points as intermediates (no imaginary frequencies) or transition states (only one imaginary frequency), as well as to obtain the sum of electronic and thermal free energies (G) at a temperature of 298 K. The most stabilized conformation was reported herein, when several different conformations were obtained. The accurate electronic energy was obtained at the theoretical level of BP86-

https://doi.org/10.1021/jacsau.4c01139
JACS Au 2025, 5, 1289–1298

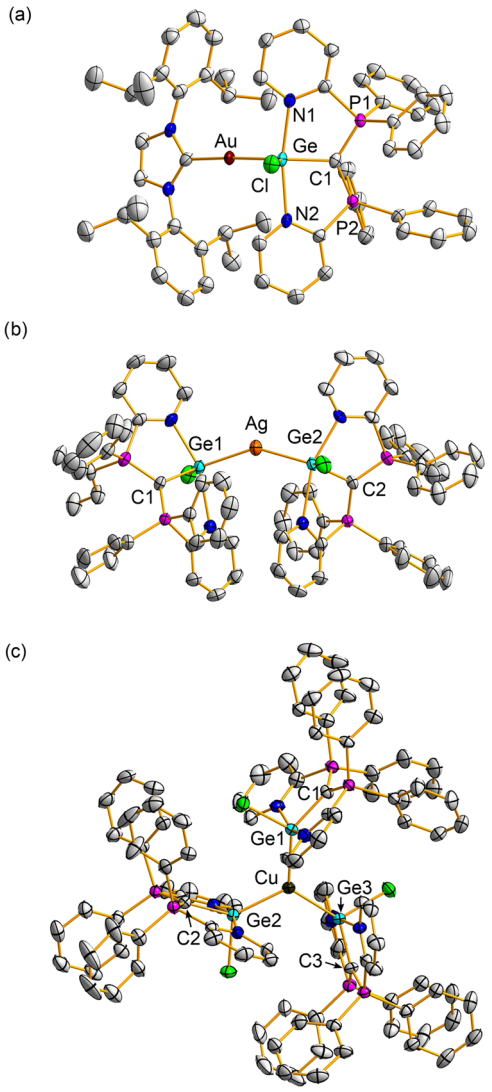

Figure 6. Molecular structures of **4**−**6**. (a) Structure of **4** in the crystal. Selected bond length (Å) and angle (deg) for **4**: C1−Ge: 1.933(7), Ge−N1: 2.216(9), Ge−N2: 2.155(9), Ge−Au: 2.338(1), C2−Au: 2.035(11), P1−C1−P2: 125.4(6), C1−Ge−Au: 133.8(3), Ge−Au−C2: 177.8(3). (b) Structure of **5** in the crystal. Selected bond length (Å) and angle (deg) for **5**: C1−Ge1: 1.974(7), Ge1−N1: 2.407(7), Ge1−N2: 2.175(7), Ge1−Ag: 2.476(1), Ag−O1: 2.537(1), Ag−O2: 2.537(1), P1−C1−P2: 125.4(4), C1−Ge1−Ag: 132.7(2), Ge1−Ag−Ge2: 146.7(2). (c) Structure of **6** in the crystal. Selected bond length (Å) and angle (deg) for **6**: C1−Ge1: 1.972(7), Ge1−N1: 2.230(7), Ge1−N2: 2.230(7), Ge1−Cu: 2.370(1), P1−C1−P2: 122.4(4), Ge1−Cu−Ge2: 120.5(4), Ge2−Cu−Ge3: 117.6(4), Ge3−Cu−Ge1: 122.0(4), C1−Ge1−Cu: 135.4(2). Hydrogen atoms, solvents, and OTf^- anions were omitted for clarity. Thermal ellipsoids are set at the 50% probability level.

D3(BJ)/def2-TZVP.[36] The mechanism calculations were performed under the IEFPCM (*o*-DCB) implicit solvent model.[37] The electron localization function (ELF) analysis and quantum theory of atoms in molecules (AIM) analysis were completed using the open-source program Multiwfn.[38] The AIM topology analysis diagrams were visualized using the Visual Molecular Dynamics (VMD) program.[39] Optimized structures were visualized by Multifwn and VMD programs.[38,39]

The natural bond orbital (NBO) analyses were performed with version 7.0, which was implemented in the G16 revision at the def2-TZVP level of theory. A03 version of the Gaussian program.[24,40] The NBO plots were visualized by the Multiwfn and VMD programs. Moreover, to gain further insight into the chemical bonding of the compounds, energy decomposition analysis (sobEDA) was performed at the BP86-D3(BJ)/def2-TZVP level using the Multiwfn program.[30] The extended transition state-natural orbitals for chemical valence (ETS-NOCV) analysis performed by Multifwn and VMD programs can investigate orbital interactions of chemical bonds between fragments.[27]

Synthesis

Compound 2Ge. $GeCl_2$·dioxane (430 mg, 1.86 mmol) was added to a suspension of $CDPPy_2$ **1** (1.00 g, 1.86 mmol) in ethyl ether (20 mL). The resulting mixture was stirred at room temperature for 12 h. The solution was filtered using a sand core funnel, and the residue solid was washed with *n*-hexane (2 × 5 mL). The solid was dried under vacuum, and the final product **2Ge** was obtained as a light yellow solid (1.05 g, yield: 73%). ^{1}H NMR (400 MHz, dichloromethane-d_2): δ = 9.05 (d, J = 5.1 Hz, 2H, *H6*), 8.16 (m, 2H, *H4*), 7.81 (m, 2H, *H5*), 7.70 (m, 2H, *H3*), 7.51 (t, J = 7.3 Hz, 4H, *H10*), 7.45−7.38 (m, 8H, *H9*), 7.33 (m, 8H, *H8*). ^{13}C NMR (101 MHz, dichloromethane-d_2): δ = 151.2−152.6 (m, *C2*), 148.3 (t, J = 7.1 Hz, *C6*), 140.3 (t, J = 4.8 Hz, *C4*), 133.8 (*C10*), 133.4 (t, J = 5.5 Hz, *C9*), 129.7 (t, J = 6.2 Hz, *C8*), 128.5 (t, J = 11.8 Hz, *C3*), 128.2 (*C5*), 125.0−126.2 (m, *C7*), 16.5 (t, J = 82.2 Hz, *C1*). ^{31}P NMR (162 MHz, dichloromethane-d_2): δ = 26.9 (s). HRMS (ESI): m/z calcd for $C_{35}H_{28}ClGeN_2P_2^+$ $[M - Cl]^+$: 647.0623, found: 647.0625.

Compound 2Sn. $SnCl_2$ (70.3 mg, 0.371 mmol) was added to a suspension of $CDPPy_2$ **1** (200 mg, 0.371 mmol) in ethyl ether (8 mL). The resulting mixture was stirred at room temperature for 12 h. The solution was filtered using a sand core funnel, and the residue solid was washed with *n*-hexane (2 × 5 mL). The collected solid was dried under vacuum, and the final product **2Sn** was obtained as an orange solid (241 mg, Yield: 89%). ^{1}H NMR (400 MHz, dichloromethane-d_2): δ = 9.08 (d, J = 5.1 Hz, 2H, *H6*), 8.11 (m, 2H, *H4*), 7.83 (m, 2H, *H5*), 7.67 (m, 2H, *H3*), 7.52 (m, 4H, *H10*), 7.41 (m, 8H, *H9*), 7.32 (m, 8H, *H8*). ^{13}C NMR (101 MHz, dichloromethane-d_2): δ = 152.5−153.9 (m, *C2*), 148.9 (t, = 7.1 Hz, *C6*), 140.2(t, J = 5.0 Hz, *C4*), 133.4 (*C10*), 133.3 (t, J = 5.3 Hz, *C9*), 129.5 (t, J = 6.2 Hz, *C8*), 129.0 (t, J = 11.7 Hz, *C3*), 126.6−127.7 (m, C7), 20.3 (t, J = 81.2 Hz, *C1*). ^{31}P NMR (162 MHz, dichloromethane-d_2): δ = 25.3 (s). ^{119}Sn NMR (149 MHz, dichloromethane-d_2): δ = −34.2 (s). HRMS (ESI): m/z calcd for $C_{35}H_{28}ClN_2P_2Sn^+$ $[M-Cl]^+$: 693.0443, found: 693.0441.

Compound 3Ge. A suspension of $CDPPy_2$ **1** (200 mg, 0.371 mmol) in ethyl ether (8 mL) was precooled at −30 °C. $GeCl_2$·dioxane (85.9 mg, 0.371 mmol) was added to the suspension and stirred for 15 min, and the color of the mixture turned from bright yellow to light yellow. Then, TMSOTf (206 mg, 0.928 mmol, 170 μL) was added dropwise to the mixture. The resulting mixture was stirred at room temperature for another 12 h. The solution was filtered using a sand core funnel, and the residue solid was washed with *n*-hexane (2 × 5 mL). The collected solid was dried under vacuum, and the final product **3Ge** was obtained as a light yellow solid (277 mg, Yield: 82%). ^{1}H NMR (400 MHz, dichloromethane-d_2): δ = 9.19 (d, J = 5.2 Hz, 2H, *H6*), 8.15 (m, 2H, *H4*), 7.88 (m, 2H, *H5*), 7.74 (m, 2H, *H3*), 7.54 (t, J_{H-H} = 7.0 Hz, 4H, *H10*), 7.42−7.46 (m, 8H, *H9*), 7.35 (m, 8H, *H8*). ^{13}C NMR (101 MHz, dichloromethane-d_2): δ = 150.6−152.2 (m, *C2*), 148.7 (t, J = 6.9 Hz, *C6*), 140.5 (t, J = 4.8 Hz, *C4*), 133.8 (*C10*), 133.0 (t, J = 5.5 Hz, *C9*), 129.5 (t, J = 6.3 Hz, *C8*), 128.4 (t, J = 11.9 Hz, *C3*), 128.3 (*C5*), 123.4−124.3 (m, *C7*), 121.7 (*C1*), 118.7 (*C11*). ^{31}P NMR (162 MHz, dichloromethane-d_2): δ = 30.4 (s). ^{19}F NMR (376 MHz, dichloromethane-d_2): δ = −78.9 (s). HRMS (ESI): m/z calcd for $C_{35}H_{28}GeN_2P_2^{2+}$ $[M - 2OTf]^{2+}$: 306.0464, found: 306.0469.

Compound 3Sn. A suspension of $CDPPy_2$ **1** (150 mg, 0.279 mmol) in ethyl ether (8 mL) was precooled at −30 °C for 2 h. $SnCl_2$ (52.8 mg, 0.279 mmol) was added to the suspension and stirred for 15 min, and the color of the mixture turned from bright yellow to light yellow. Then, TMSOTf (155 mg, 0.698 mmol, 0.13 mL) was added dropwise to the mixture. The resulting mixture was stirred at room temperature for 12 h. The solution was filtered using a sand

https://doi.org/10.1021/jacsau.4c01139
JACS Au 2025, 5, 1289−1298

core funnel, and the residue solid was washed with *n*-hexane (2 × 5 mL). The collected solid was dried under vacuum and obtained as a pale yellow mixture with **3Sn** (yield: 33% by NMR analysis). ^{1}H NMR (400 MHz, dichloromethane-d_2): δ = 9.16 (d, J = 5.1 Hz, 2H, *H6*), 8.07 (m, 2H, *H4*), 7.86 (t, J = 6.6 Hz, 2H, *H5*), 7.65 (m, 2H, *H3*), 7.46 (m, 12H, *H10* and *H9*), 7.32 (m, 8H, *H8*). ^{13}C NMR (101 MHz, dichloromethane-d_2): δ = 152.8−154.2 (m, *C2*), 149.4 (t, J = 6.8 Hz, *C6*), 140.3 (t, J = 5.0 Hz, *C4*), 133.6 (s, *C10*), 133.5 (t, J = 5.4 Hz, *C9*), 129.7 (t, J = 6.3 Hz, *C8*), 129.4 (s, *C5*), 129.3 (t, J = 12.0 Hz, *C3*), 125.8−126.8 (m, *C7*), 125.6 (*C1*), 115.1 (*C11*). ^{31}P NMR (162 MHz, dichloromethane-d_2): δ = 28.6 (s). ^{19}F NMR (376 MHz, dichloromethane-d_2): δ = −78.8 (s) ^{119}Sn NMR (149 MHz, dichloromethane-d_2): δ = −87.9 (s) HRMS (ESI): m/z calcd for $C_{35}H_{29}N_2P_2^+$ $[M - SnOTf_2 + H]^+$: 539.1805, found: 539.1759.

Compound 4. NHC^{Dipp} → AuCl (68.3 mg, 0.110 mmol) was added to a solution of **3Ge** (100 mg, 0.110 mmol) in orthodichlorobenzene (6 mL) at room temperature. The resulting mixture was stirred for 12 h. DCM (10 mL) was then added to the mixture, and all volatile components were removed under vacuum. The residue solid was washed twice with *n*-hexane (2 × 5 mL). The solid was then dried under vacuum, and the final product **4** was obtained as a colorless solid (135 mg, yield: 80%). ^{1}H NMR (400 MHz, dichloromethane-d_2): δ = 8.40 (td, J = 7.8, 2.5 Hz, 2H, *H6*), 8.28 (d, J = 5.2 Hz, 2H, *H4*), 7.99 (m, 2H, *H3*), 7.74 (t, J = 6.6 Hz, 2H, *H5*), 7.62 (t, J = 7.7 Hz, 4H, *H15*), 7.49 (m, 3H, *Dipp-H*), 7.38 (m, 6H, *H10* and *H12*), 7.31 (m, 10H, *Ph-H*), 7.22 (m, 5H, *Dipp-H* and *Ph-H*), 2.45 (p, J = 6.9 Hz, 4H, *H17*), 1.23 (d, J = 6.8 Hz, 12H, *H19/H18*), 1.10 (d, J = 6.8 Hz, 12H, *H18/H19*). ^{13}C NMR (101 MHz, dichloromethane-d_2): δ = 190.8 (*C20*), 146.3 (*C4*), 143.9−145.2 (*C2*), 143.0 (*C6*), 135.1 (*C-Dipp*), 133.7 (*C10*), 133.6 (*C9*), 132.9 (*C-Dipp*), 132.7 (*C-Dipp*), 131.9 (*C8*), 130.9 (*C-Dipp*), 130.5 (*C5*), 130.2 (*C3*), 128.3 (*C-Dipp*), 124.8 (*C12*), 122.7−123.0 (*C7*), 121.3 (*C1*), 29.2 (*C17*), 25.3 (*C18/C19*), 23.9 (*C18/C19*). *C11* is not detected or is masked by other peaks. ^{31}P NMR (162 MHz, dichloromethane-d_2): δ = 22.1 (s). ^{19}F NMR (376 MHz, dichloromethane-d_2): δ = −78.8 (s). HRMS (ESI): m/z calcd for $C_{62}H_{64}AuClGeN_4P_2$ $[M - 2OTf]^{2+}$: 616.1581, found: 616.1661.

Compound 5. NHC^{Dipp} → AgCl (58.6 mg, 0.11 mmol) was added to a solution of **3Ge** (100 mg, 0.11 mmol) in orthodichlorobenzene (5 mL) at room temperature. The resulting mixture was stirred for 12 h. DCM (10 mL) was then added to the mixture, and all volatile components were removed under vacuum. The residue solid was washed twice with *n*-hexane (2 × 5 mL). The solid was then dried under vacuum, and the final product **5** was obtained as a yellow solid (64.1 mg, yield: 63%). ^{1}H NMR (400 MHz, dichloromethane-d_2): δ = 8.48 (d, J = 5.3 Hz, 2H, *H6*), 8.09 (m, 2H, *H4*), 7.80 (m, 2H, *H5*), 7.65 (2H, *H3*), 7.35−7.56 (m, 20H, H8, H9, H10). ^{13}C NMR (101 MHz, dichloromethane-d_2): δ = 147.1−148.4 (m, *C2*), 147.7 (t, J = 6.9 Hz, *C6*), 141.6 (t, J = 4.8 Hz, *C4*), 134.6 (*C10*), 134.0 (*C9*), 129.8−130.3 (*C8*), 129.0 (C5), 128.3 (t, J = 10.9 Hz, *C3*), 123.3−124.6 (m, *C7*), 122.9 (*C1*), 119.7 (*C11*). ^{31}P NMR (162 MHz, dichloromethane-d_2): δ = 25.7 (s). ^{19}F NMR (372 MHz, dichloromethane-d_2): δ = −78.5 (s).

Compound 6. NHC^{Dipp} → CuCl (53.6 mg, 0.11 mmol) was added to a solution of **3Ge** (100.0 mg, 0.11 mmol) in *ortho*-dichlorobenzene (5 mL) at room temperature. The resulting mixture was stirred for 12 h. DCM (10 mL) was then added to the mixture, and all volatile components were removed under vacuum. The residue solid was washed twice with *n*-hexane (2 × 5 mL). The solid was then dried under vacuum, and the final product **6** was obtained as a yellow solid (61.9 mg, yield: 65%). ^{1}H NMR (400 MHz, dichloromethane-d_2): δ = 8.80 (br, 6H, *H6*), 8.10 (m, 6H, *H4*), 7.77 (m, 6H, *H5*), 7.58 (br, 6H, *H3*), 7.50 (m, 36H, C10, C9), 7.38 (m, 24H, C8). ^{13}C NMR (101 MHz, dichloromethane-d_2): δ = 146.2−149.7 (m, *C2*), 148.2 (t, J = 6.9 Hz, *C6*), 141.1 (*C4*), 134.3 (*C10*), 133.7 (t, J = 5.7 Hz, *C9*), 129.9 (t, J = 6.4 Hz, *C8*), 128.7 (*C5*), 128.6 (t, J = 11.1 Hz, *C3*), 123.9−125.1 (m, *C7*), 122.6 (*C1*), 119.4 (*C11*). ^{31}P NMR (162 MHz, dichloromethane-d_2): δ = 26.9 (s). ^{19}F NMR (376 MHz, dichloromethane-d_2): δ = −78.7 (s).

■ ASSOCIATED CONTENT

Supporting Information

The Supporting Information is available free of charge at https://pubs.acs.org/doi/10.1021/jacsau.4c01139.

Synthetic details, crystallographic data, full characterization data (e.g., NMR, HRMS, etc.), and computational details (PDF)

■ AUTHOR INFORMATION

Corresponding Author

Zhaowen Dong − *Key Laboratory of Green Chemistry & Technology, Ministry of Education, College of Chemistry, Sichuan University, Chengdu 610064, P. R. China;* orcid.org/0000-0001-6163-470X; Email: dongzhaowen@scu.edu.cn

Authors

Yuankai Li − *Key Laboratory of Green Chemistry & Technology, Ministry of Education, College of Chemistry, Sichuan University, Chengdu 610064, P. R. China*

Huan Mu − *Key Laboratory of Green Chemistry & Technology, Ministry of Education, College of Chemistry, Sichuan University, Chengdu 610064, P. R. China*

Zhuchunguang Liu − *Key Laboratory of Green Chemistry & Technology, Ministry of Education, College of Chemistry, Sichuan University, Chengdu 610064, P. R. China*

Zexin Qi − *Key Laboratory of Green Chemistry & Technology, Ministry of Education, College of Chemistry, Sichuan University, Chengdu 610064, P. R. China*

Jiliang Zhou − *Key Laboratory of Green Chemistry & Technology, Ministry of Education, College of Chemistry, Sichuan University, Chengdu 610064, P. R. China;* orcid.org/0000-0002-1857-6206

Complete contact information is available at: https://pubs.acs.org/10.1021/jacsau.4c01139

Author Contributions

†Y.L., H.M., and Z.L. contributed equally to this work. The manuscript was written through contributions of all authors. All authors have given approval to the final version of the manuscript.

Notes

The authors declare no competing financial interest.

■ ACKNOWLEDGMENTS

This work was financially supported by the National Key R&D Program of China (2023YFC3903200), the National Natural Science Foundation of China (22471176), the Natural Science Foundation of Sichuan, China (2023NSFSC1083), the Fundamental Research Funds for the Central Universities (YJ202269), and the Institutional Research Fund from Sichuan University (2024SCUQJTX006). The authors thank Drs. Jing Li, Dongyan Deng, and Meng Yang from the College of Chemistry at Sichuan University for their suggestions and assistance in HRMS, NMR, and sc-XRD analyses. The authors thank Dr. Pengchi Deng from the Analytical & Testing Center at Sichuan University for the NMR support. The authors also thank Prof. Thomas Müller from Carl von Ossietzky University Oldenburg for his valuable comments and suggestions.

REFERENCES

(1) (a) Davis, J. H.; Goddard, W. A.; Harding, L. B. Theoretical studies of the low-lying states of vinylidene. *J. Am. Chem. Soc.* **1977**, *99*, 2919−2925. (b) Kenney, J. W.; Simons, J.; Purvis, G. D.; Bartlett, R. J. Low-lying electronic states of unsaturated carbenes. Comparison with methylene. *J. Am. Chem. Soc.* **1978**, *100*, 6930−6936. (c) Gallo, M. M.; Hamilton, T. P.; Schaefer, H. F. Vinylidene: the final chapter? *J. Am. Chem. Soc.* **1990**, *112*, 8714−8719. (d) Kutin, Y.; Reitz, J.; Antoni, P. W.; Savitsky, A.; Pantazis, D. A.; Kasanmascheff, M.; Hansmann, M. M. Characterization of a Triplet Vinylidene. *J. Am. Chem. Soc.* **2021**, *143*, 21410−21415.

(2) (a) Stang, P. J. Unsaturated carbenes. *Chem. Rev.* **1978**, *78*, 383−405. (b) Bruce, M. I. Organometallic chemistry of vinylidene and related unsaturated carbenes. *Chem. Rev.* **1991**, *91*, 197−257. (c) Knorr, R. Alkylidenecarbenes, Alkylidenecarbenoids,† and Competing Species: Which Is Responsible for Vinylic Nucleophilic Substitution, [1 + 2] Cycloadditions, 1,5−CH Insertions, and the Fitsch−Buttenberg−Wiechell Rearrangement? *Chem. Rev.* **2004**, *104*, 3795−3850.

(3) (a) Brody, H. K.; Magers, D. H.; Leszczyński, J. Ab initio studies of methylenecarbene and isoelectronic species. *Struct. Chem.* **1995**, *6*, 293−300. (b) O'Leary, P.; Thomas, J. R.; Schaefer, H. F.; Duke, B. J.; O'Leary, B. A study of the silagermylyne ($SiGeH_2$) molecule: A new monobridged structure. *Int. J. Quantum Chem.* **1995**, *56*, 593−604. (c) Boone, A. J.; Magers, D. H.; Leszczyński, J. Searches on the potential energy hypersurfaces of $GeCH_2$, $GeSiH_2$, and Ge_2H_2. *Int. J. Quantum Chem.* **1998**, *70*, 925−932. (d) Nagase, S.; Kobayashi, K.; Takagi, N. Triple bonds between heavier Group 14 elements. A theoretical approach. *J. Organomet. Chem.* **2000**, *611*, 264−271. (e) Lein, M.; Krapp, A.; Frenking, G. Why Do the Heavy-Atom Analogues of Acetylene E_2H_2 (E = Si−Pb) Exhibit Unusual Structures? *J. Am. Chem. Soc.* **2005**, *127*, 6290−6299.

(4) Jana, A.; Huch, V.; Scheschkewitz, D. NHC-Stabilized Silagermenylidene: A Heavier Analogue of Vinylidene. *Angew. Chem., Int. Ed.* **2013**, *52*, 12179−12182.

(5) (a) Leung, W.-P.; Chan, Y.-C.; So, C.-W. Chemistry of Heavier Group 14 Base-Stabilized Heterovinylidenes. *Organometallics* **2015**, *34*, 2067−2085. (b) Rivard, E. Group 14 inorganic hydrocarbon analogues. *Chem. Soc. Rev.* **2016**, *45*, 989−1003. (c) Weetman, C. Main Group Multiple Bonds for Bond Activations and Catalysis. *Chem.—Eur. J.* **2021**, *27*, 1941−1954. (d) Ota, K.; Kinjo, R. Zerovalent species of group 13−15 elements. *Chem* **2022**, *8*, 340−350.

(6) (a) Ghana, P.; Arz, M. I.; Das, U.; Schnakenburg, G.; Filippou, A. C. Si = Si Double Bonds: Synthesis of an NHC-Stabilized Disilavinylidene. *Angew. Chem., Int. Ed.* **2015**, *54*, 9980−9985. (b) Kobayashi, R.; Ishida, S.; Iwamoto, T. Synthesis of an NHC-Coordinated Dialkyldisilavinylidene and Its Oxidation Providing a Silicon Analog of an Acetolactone. *Organometallics* **2021**, *40*, 843−847. (c) Qiao, Z.; Chen, M.; Mo, Z. A silylene-stabilized distannavinylidene with a highly labile substituent. *Sci. China Chem.* **2023**, *66*, 3555−3561. (d) Qiao, Z.; Li, X.; Chen, M.; Cao, F.; Mo, Z. Double 1,2-Carbon Migration at Mixed Heavier Sn = Ge Vinylidenes. *Angew. Chem., Int. Ed.* **2024**, *63*, No. e202401570. (e) Krebs, K. M.; Hanselmann, D.; Schubert, H.; Wurst, K.; Scheele, M.; Wesemann, L. Phosphine-Stabilized Digermavinylidene. *J. Am. Chem. Soc.* **2019**, *141*, 3424−3429. (f) Wilhelm, C.; Raiser, D.; Schubert, H.; Sindlinger, C. P.; Wesemann, L. Phosphine-Stabilized Germasilenylidene: Source for a Silicon-Atom Transfer. *Inorg. Chem.* **2021**, *60*, 9268−9272.

(7) Rit, A.; Campos, J.; Niu, H.; Aldridge, S. A stable heavier group 14 analogue of vinylidene. *Nat. Chem.* **2016**, *8*, 1022−1026.

(8) (a) Sherrill, C. D.; Schaefer, H. F., III 1-Silavinylidene: The First Unsaturated Silylene. *J. Phys. Chem. A* **1995**, *99*, 1949−1952. (b) Ayoubi-Chianeh, M.; Kassaee, M. Z. Novel triplet silavinylidenes via density functional theory. *J. Phys. Org. Chem.* **2020**, *33*, No. e4074. (c) Stogner, S. M.; Grev, R. S. Germyne, H−C≡Ge−H, and the excited states of 1-germavinylidene, H_2C = Ge. *J. Chem. Phys.* **1998**, *108*, 5458−5464. (d) Hao, Q.; Lu, T.; Wilke, J. J.; Simmonett, A. C.; Yamaguchi, Y.; Fang, D.-C.; Schaefer, H. F. 1-Germavinylidene (Ge = CH_2), Germyne (HGeCH), and 2-Germavinylidene (H_2Ge = C) Molecules and Isomerization Reactions among Them: Anharmonic Rovibrational Analyses. *J. Phys. Chem. A* **2012**, *116*, 4578−4589.

(9) (a) Leung, W.-P.; Chiu, W.-K.; Mak, T. C. W. Synthesis and Structural Characterization of Base-Stabilized Oligomeric Heterovinylidenes. *Inorg. Chem.* **2013**, *52*, 9479−9486. (b) Guo, J.; Lau, K.-C.; Xi, H.-W.; Lim, K. H.; So, C.-W. Synthesis and characterization of a tin(II) bis(phosphinoyl)methanediide complex: a stannavinylidene derivative. *Chem. Commun.* **2010**, *46*, 1929−1931. (c) Leung, W.-P.; So, C.-W.; Kan, K.-W.; Chan, H.-S.; Mak, T. C. W. Synthesis of a Manganese Germavinylidene Complex from Bis(germavinylidene). *Inorg. Chem.* **2005**, *44*, 7286−7288. (d) Leung, W.-P.; So, C.-W.; Wang, Z.-X.; Wang, J.-Z.; Mak, T. C. W. Synthesis of Bisgermavinylidene and Its Reaction with Chalcogens. *Organometallics* **2003**, *22*, 4305−4311. (e) Leung, W.-P.; Wang, Z.-X.; Li, H.-W.; Mak, T. C. W. Bis(germavinylidene) [$(Me_3SiN = PPh_2)_2$ C = Ge→Ge = C(Ph_2 P = $NSiMe_3$)] and 1,3-Dimetallacyclobutanes [$M\{\mu^2$-C(Ph_2 P = $NSiMe_3)_2\}]_2$ (M = Sn, Pb). *Angew. Chem., Int. Ed.* **2001**, *40*, 2501−2503.

(10) Li, Y.; Chan, Y.-C.; Li, Y.; Purushothaman, I.; De, S.; Parameswaran, P.; So, C.-W. Synthesis of a Bent 2-Silaallene with a Perturbed Electronic Structure from a Cyclic Alkyl(amino) Carbene-Diiodosilylene. *Inorg. Chem.* **2016**, *55*, 9091−9098.

(11) Sarcevic, J.; Heitkemper, T.; Ruth, P. N.; Naß, L.; Kubis, M.; Stalke, D.; Sindlinger, C. P. A donor-supported silavinylidene and silylium ylides: boroles as a flexible platform for versatile Si(II) chemistry. *Chem. Sci.* **2023**, *14*, 5148−5159.

(12) Kumar, S.; Maurer, L. R.; Schnakenburg, G.; Das, U.; Filippou, A. C. NHC-Supported 2-Sila and 2-Germavinylidenes: Synthesis, Dynamics, First Reactivity and Theoretical Studies. *Angew. Chem., Int. Ed.* **2024**, *63*, No. e202400227.

(13) (a) Johansen, M. A. L.; Ghosh, A. The curious chemistry of carbones. *Nat. Chem.* **2023**, *15*, 1042. (b) Liberman-Martin, A. L. The emergence of zerovalent carbon compounds from structural curiosities to organocatalysts. *Cell Rep. Phys. Sci.* **2023**, *4*, No. 101519. (c) Liu, S-k.; Shih, W.-C.; Chen, W.-C.; Ong, T.-G. Carbodicarbenes and their Captodative Behavior in Catalysis. *ChemCatChem* **2018**, *10*, 1483−1498. (d) Frenking, G.; Tonner, R.; Klein, S.; Takagi, N.; Shimizu, T.; Krapp, A.; Pandey, K. K.; Parameswaran, P. New bonding modes of carbon and heavier group 14 atoms Si−Pb. *Chem. Soc. Rev.* **2014**, *43*, 5106−5139. (e) Frenking, G.; Hermann, M.; Andrada, D. M.; Holzmann, N. Donor-acceptor bonding in novel low-coordinated compounds of boron and group-14 atoms C−Sn. *Chem. Soc. Rev.* **2016**, *45*, 1129−1144.

(14) (a) Inés, B.; Patil, M.; Carreras, J.; Goddard, R.; Thiel, W.; Alcarazo, M. Synthesis, Structure, and Reactivity of a Dihydrido Borenium Cation. *Angew. Chem., Int. Ed.* **2011**, *50*, 8400−8403. (b) Khan, S.; Gopakumar, G.; Thiel, W.; Alcarazo, M. Stabilization of a Two-Coordinate $GeCl^+$ Cation by Simultaneous σ and π Donation from a Monodentate Carbodiphosphorane. *Angew. Chem., Int. Ed.* **2013**, *52*, 5644−5647. (c) Su, W.; Ma, Y.; Xiang, L.; Wang, J.; Wang, S.; Zhao, L.; Frenking, G.; Ye, Q. Isolation of a Uranium(III)-Carbon Multiple Bond Complex. *Chem.—Eur. J.* **2021**, *27*, 10006−10011. (d) Xiang, L.; Wang, J.; Su, W.; Lin, Z.; Ye, Q. Facile access to halogenated cationic B = C-centered organoborons isoelectronic with alkenyl halides. *Dalton Trans.* **2021**, *50*, 17491−17494. (e) Su, W.; Pan, S.; Sun, X.; Wang, S.; Zhao, L.; Frenking, G.; Zhu, C. Double dative bond between divalent carbon(0) and uranium. *Nat. Commun.* **2018**, *9*, No. 4997. (f) Fang, W.; Pan, S.; Su, W.; Wang, S.; Zhao, L.; Frenking, G.; Zhu, C. Complex Featuring Two Double Dative Bonds Between Carbon(0) and Uranium. *CCS Chem.* **2022**, *4*, 1921−1929.

(15) (a) Warring, L.; Westendorff, K. S.; Bennett, M. T.; Nam, K.; Stewart, B. M.; Dickie, D. A.; Paolucci, C.; Gunnoe, T. B.; Gilliard, R. J., Jr. Carbodicarbene-Stibenium Ion-Mediated Functionalization of C(sp3)−H and C(sp)−H Bonds. *Angew. Chem., Int. Ed.* **2024**, No. e202415070. (b) Obi, A. D.; Deng, C.-L.; Alexis, A. J.; Dickie, D. A.; Gilliard, R. J., Jr. Geminal bimetallic coordination of a carbone to main-group and transition metals. *Chem. Commun.* **2024**, *60*, 1880−1883. (c) Hollister, K. K.; Molin, A.; Breiner, G.; Walley, J. E.; Wentz, K. E.; Conley, A. M.; Dickie, D. A.; Wilson, J. D.; Gilliard, R. J., Jr. Air-

https://doi.org/10.1021/jacsau.4c01139
JACS Au 2025, 5, 1289−1298

Stable Thermoluminescent Carbodicarbene-Borafluorenium Ions. *J. Am. Chem. Soc.* **2022**, *144*, 590−598. (d) Warring, L. S.; Walley, J. E.; Dickie, D. A.; Tiznado, W.; Pan, S.; Gilliard, R. J., Jr. Lewis Superacidic Heavy Pnictaalkene Cations: Comparative Assessment of Carbodicarbene-Stibenium and Carbodicarbene-Bismuthenium Ions. *Inorg. Chem.* **2022**, *61*, 18640−18652. (e) Walley, J. E.; Warring, L. S.; Wang, G.; Dickie, D. A.; Pan, S.; Frenking, G.; Gilliard, R. J., Jr. Carbodicarbene Bismaalkene Cations: Unravelling the Complexities of Carbene versus Carbone in Heavy Pnictogen Chemistry. *Angew. Chem., Int. Ed.* **2021**, *60*, 6682−6690. (f) Buchner, M. R.; Pan, S.; Poggel, C.; Spang, N.; Mueller, M.; Frenking, G.; Sundermeyer, J. Di-*ortho*-beryllated Carbodiphosphorane: A Compound with a Metal Carbon Double Bond to an Element of the s-Block. *Organometallics* **2020**, *39*, 3224−3231.

(16) Klein, M.; Xie, X.; Burghaus, O.; Sundermeyer, J. Synthesis and Characterization of a *N,C,N*-Carbodiphosphorane Pincer Ligand and Its Complexes. *Organometallics* **2019**, *38*, 3768−3777.

(17) (a) Lee, V. Y.; Sekiguchi, A. Heteronuclear heavy alkenes E = E′ (E, E′ = group 14 elements): Germasilenes, silastannenes, germastannenes···: Next stop? *Organometallics* **2004**, *23*, 2822−2834. (b) Lee, V. Y. *Organogermanium Compounds: Theory, Experiment, and Applications*; Lee, V. Y., Ed.; John Wiley & Sons, 2023; Vol. *1*, pp 435−475.

(18) (a) Glavinović, M.; Krause, M.; Yang, L.; McLeod, J. A.; Liu, L.; Baines, K. M.; Friščić, T.; Lumb, J.-P. A chlorine-free protocol for processing germanium. *Sci. Adv.* **2017**, *3*, No. e1700149. (b) Ruddy, A. J.; Rupar, P. A.; Bladek, K. J.; Allan, C. J.; Avery, J. C.; Baines, K. M. On the Bonding in N-Heterocyclic Carbene Complexes of Germanium(II). *Organometallics* **2010**, *29*, 1362−1367. (c) Henry, A. T.; Cosby, T. P. L.; Boyle, P. D.; Baines, K. M. Selective dimerization of α-methylstyrene by tunable bis(catecholato)germane Lewis acid catalysts. *Dalton Trans.* **2021**, *50*, 15906−15913.

(19) (a) Rupar, P. A.; Staroverov, V. N.; Baines, K. M. A Cryptand-Encapsulated Germanium(II) Dication. *Science* **2008**, *322*, 1360−1363. (b) Rupar, P. A.; Jennings, M. C.; Baines, K. M. Synthesis and Structure of N-heterocyclic Carbene Complexes of Germanium(II). *Organometallics* **2008**, *27*, 5043−5051.

(20) (a) Majumdar, M.; Raut, R. K.; Sahoo, P.; Kumar, V. Bis(chlorogermyliumylidene) and its significant role in elusive reductive cyclization. *Chem. Commun.* **2018**, *54*, 10839−10842. (b) Dias, H. V. R.; Wang, Z. Germanium-containing heterobicyclic 10-π-Electron Ring Systems. Synthesis and Characterization of Neutral and Cationic Germanium(II) Derivatives of Aminotroponiminates. *J. Am. Chem. Soc.* **1997**, *119*, 4650−4655.

(21) (a) Stigler, S.; Fujimori, S.; Kostenko, A.; Inoue, S. Tetryliumylidene ions in synthesis and catalysis. *Chem. Sci.* **2024**, *15*, 4275−4291. (b) Jambor, R.; Novák, M. Low Valent N-Coordinated Cations and Dications of Heavier Group 14 Elements: Lewis Acids or Bases? *Eur. J. Inorg. Chem.* **2023**, *26*, No. e202300505. (c) Biswas, S.; Patel, N.; Deb, R.; Majumdar, M. Chemistry of the Bis(imine)-Based Tetradentate Ligand Stabilized Group 14 E(II) Cations (E = Ge and Sn). *Chem. Rec.* **2022**, *22*, No. e202200003.

(22) Pyykkö, P.; Atsumi, M. Molecular Double-Bond Covalent Radii for Elements Li-E112. *Chem.—Eur. J.* **2009**, *15*, 12770−12779.

(23) Frisch, M. J.; Trucks, G. W.; Schlegel, H. B.; Scuseria, G. E.; Robb, M. A.; Cheeseman, J. R.; Scalmani, G.; Barone, V.; Petersson, G. A.; Nakatsuji, H.; Li, X.; Caricato, M.; Marenich, A. V.; Bloino, J.; Janesko, B. G.; Gomperts, R.; Mennucci, B.; Hratchian, H. P.; Ortiz, J. V.; Izmaylov, A. F.; Sonnenberg, J. L.; Williams-Young, D.; Ding, F.; Lipparini, F.; Egidi, F.; Goings, J.; Peng, B.; Petrone, A.; Henderson, T.; Ranasinghe, D.; Zakrzewski, V. G.; Gao, J.; Rega, N.; Zheng, G.; Liang, W.; Hada, M.; Ehara, M.; Toyota, K.; Fukuda, R.; Hasegawa, J.; Ishida, M.; Nakajima, T.; Honda, Y.; Kitao, O.; Nakai, H.; Vreven, T.; Throssell, K.; Montgomery, J. A., Jr.; Peralta, J. E.; Ogliaro, F.; Bearpark, M. J.; Heyd, J. J.; Brothers, E. N.; Kudin, K. N.; Staroverov, V. N.; Keith, T. A.; Kobayashi, R.; Normand, J.; Raghavachari, K.; Rendell, A. P.; Burant, J. C.; Iyengar, S. S.; Tomasi, J.; Cossi, M.; Millam, J. M.; Klene, M.; Adamo, C.; Cammi, R.; Ochterski, J. W.; Martin, R. L.; Morokuma, K.; Farkas, O.; Foresman, J. B.; Fox, D. J. *Gaussian 16*, revision A.03; Gaussian, Inc.: Wallingford CT, 2016.

(24) Glendening, E. D.; Badenhoop, J. K.; Bohmann, J. A.; Morales, C. M.; Karafiloglou, P.; Landis, C. R.; Weinhold, F. *NBO 7.0*; Theoretical Chemistry Institute, University of Wisconsin: Madison, WI, 2018.

(25) Hu, C.; Wang, X.-F.; Li, J.; Chang, X.-Y.; Liu, L. L. A stable rhodium-coordinated carbene with a $\sigma^0\pi^2$ electronic configuration. *Science* **2024**, *383*, 81−85.

(26) Wiberg, K. B. Application of the pople-santry-segal CNDO method to the cyclopropylcarbinyl and cyclobutyl cation and to bicyclobutane. *Tetrahedron* **1968**, *24*, 1083−1109.

(27) Mitoraj, M. P.; Michalak, A.; Ziegler, T. A Combined Charge and Energy Decomposition Scheme for Bond Analysis. *J. Chem. Theory Comput.* **2009**, *5*, 962−975.

(28) Bader, R. F. *Atoms in Molecules: A Quantum Theory*; Clarendon Press: Oxford, U.K., 1990.

(29) Savin, A.; Nesper, R.; Wengert, S.; Fässler, T. F. ELF: The electron localization function. *Angew. Chem., Int. Ed.* **1997**, *36*, 1809−1832.

(30) Lu, T.; Chen, Q. Simple, Efficient, and Universal Energy Decomposition Analysis Method Based on Dispersion-Corrected Density Functional Theory. *J. Phys. Chem. A* **2023**, *127*, 7023−7035.

(31) Ghosh, M.; Sen, N.; Khan, S. Coinage Metal Complexes of Germylene and Stannylene. *ACS Omega* **2022**, *7*, 6449−6454.

(32) Dolomanov, O. V.; Bourhis, L. J.; Gildea, R. J.; Howard, J. A. K.; Puschmann, H. *OLEX2*: a complete structure solution, refinement and analysis program. *J. Appl. Crystallogr.* **2009**, *42*, 339−341.

(33) Sheldrick, G. M. *SHELXT* - Integrated space-group and crystal-structure determination. *Acta Crystallogr., Sect. A: Found. Adv.* **2015**, *71*, 3−8.

(34) Perdew, J. P. Density-functional approximation for the correlation energy of the inhomogeneous electron gas. *Phys. Rev. B* **1986**, *33*, 8822−8824.

(35) Grimme, S. Accurate description of van der Waals complexes by density functional theory including empirical corrections. *J. Comput. Chem.* **2004**, *25*, 1463−1473.

(36) Weigend, F.; Ahlrichs, R. Balanced basis sets of split valence, triple zeta valence and quadruple zeta valence quality for H to Rn: Design and assessment of accuracy. *Phys. Chem. Chem. Phys.* **2005**, *7*, 3297−3305.

(37) Miertuš, S.; Scrocco, E.; Tomasi, J. Electrostatic interaction of a solute with a continuum. A direct utilizaion of AB initio molecular potentials for the prevision of solvent effects. *Chem. Phys.* **1981**, *55*, 117−129.

(38) Lu, T.; Chen, F. Multiwfn: A multifunctional wavefunction analyzer. *J. Comput. Chem.* **2012**, *33*, 580−592.

(39) Humphrey, W.; Dalke, A.; Schulten, K. VMD: Visual molecular dynamics. *J. Mol. Graphics* **1996**, *14*, 33−38.

(40) Reed, A. E.; Curtiss, L. A.; Weinhold, F. Intermolecular interactions from a natural bond orbital, donor-acceptor viewpoint. *Chem. Rev.* **1988**, *88*, 899−926.

https://doi.org/10.1021/jacsau.4c01139
JACS Au 2025, 5, 1289−1298